HITACHI

GE Hitachi Nuclear Energy

Richard E. Kingston
Vice President, ESBWR Licensing

P.O. Box 780
3901 Castle Hayne Road, M/C A-55
Wilmington, NC 28402 USA

T 910.675.6192
F 910.362.6192
rick.kingston@ge.com

MFN 06-191
Supplement 8

Docket No. 52-010

September 8, 2008

U.S. Nuclear Regulatory Commission
Document Control Desk
Washington, D.C. 20555-0001

Subject: Response to Portion of NRC Request for Additional Information Letter No. 166 Related to ESBWR Design Certification Application – Seismic Category I Structures – RAI Number 3.8-25 S05

The purpose of this letter is to submit the GE Hitachi Nuclear Energy (GEH) response to a portion of the U.S. Nuclear Regulatory Commission (NRC) Request for Additional Information (RAI) sent by NRC letter dated March 28, 2008 (Reference 1). The original RAI and the GEH responses are listed in References 2 through 7.

RAI Number 3.8-25, Supplement 5 is addressed in Enclosure 1. Additional information supporting this response is provided in Attachment 1.

If you have any questions or require additional information, please contact me.

Sincerely,

Richard E. Kingston

Richard E. Kingston
Vice President, ESBWR Licensing

D068
NRO

References:

1. MFN 08-316, Letter from U. S. Nuclear Regulatory Commission to Mr. Robert E. Brown, *Request for Additional Information Letter No. 166 Related to ESBWR Design Certification Application*, March 28, 2008

2. MFN 06-191, Supplement 6, Letter from James C. Kinsey to U.S. Nuclear Regulatory Commission, *Response to Portion of NRC Request for Additional Information Letter No. 38 Related to ESBWR Design Certification Application – Structural Analysis – RAI Numbers 3.8-25 S04, 3.8-41 S04 and 3.8-91 S04*, December 12, 2007

3. MFN 06-191, Supplement 3, Letter from James C. Kinsey to U.S. Nuclear Regulatory Commission, *Response to Portion of RAI Letter No. 38 Related to ESBWR Design Certification Application - Seismic Category I Structures – RAI Numbers 3.8-3 S03, 3.8-6 S02, 3.8-13 S03, 3.8-14 S02, 3.8-18 S02, 3.8-20 S01, 3.8-25 S03, 3.8-26 S01, 3.8-27 S02, 3.8-41 S03, 3.8-46 S02, 3.8-48 S03, 3.8-51 S03, 3.8-56 S01, 3.8-64 S03, 3.8-87 S02, 3.8-90 S02, 3.8-91 S03 & 3.8-100 S02- Supplement 3*, January 24, 2007

4. MFN 06-191, Supplement 2, Letter from David Hinds to U.S. Nuclear Regulatory Commission, *Response to Portion of RAI Letter No. 38 Related to ESBWR Design Certification Application - Seismic Category I Structures – RAI Numbers 3.8-3, 3.8-13, 3.8-25, 3.8-41, 3.8-48, 3.8-51, 3.8-64, and 3.8-91- Supplement 2*, November 7, 2006

5. MFN 06-191, Supplement 1, Letter from David Hinds to U.S. Nuclear Regulatory Commission, *Response to Portion of RAI Letter No. 38 Related to ESBWR Design Certification Application - Seismic Category I Structures – RAI Numbers 3.8-3, 3.8-6, 3.8-13, 3.8-14, 3.8-18, 3.8-25, 3.8-27, 3.8-46, 3.8-48, 3.8-63, 3.8-64, 3.8-82, 3.8-87, 3.8-90, 3.8-91, 3.8-100, 3.8-104, and 3.8-106 - Supplement 1*, September 14, 2006

6. MFN 06-191, Letter from David Hinds to U.S. Nuclear Regulatory Commission, *Response to Portion of NRC Request for Additional Information Letter No. 38 Related to ESBWR Design Certification Application – Structural Analysis - RAI Numbers 3.8 3, 3.8 6, 3.8 13, 3.8 14, 3.8 18, 3.8 19, 3.8 20, 3.8 23, 3.8 25, 3.8 26, 3.8 27, 3.8 40, 3.8 41, 3.8 46, 3.8 47, 3.8 48, 3.8 49, 3.8 51, 3.8 56, 3.8 63, 3.8 64, 3.8 82, 3.8 83, 3.8 87, 3.8 90, 3.8 91, 3.8 100, 3.8 104, 3.8 105 and 3.8 106*, June 28, 2006

7. MFN 06-197, Letter from U. S. Nuclear Regulatory Commission to Mr. David H. Hinds, *Request for Additional Information Letter No. 38 Related to ESBWR Design Certification Application*, June 23, 2006

Enclosure:

1. Response to Portion of NRC RAI Letter No. 166 Related to ESBWR Design Certification Application, DCD Tier 2 Section 3.8 – Seismic Category I Structures – RAI Number 3.8-25 S05

Attachment:

1. Attachment 3.8-25(1), A. Komori, M. Nazuka, 0. Oyamada, H, Furukawa, M. Hiroshima, Y. Muramatsu, M. Hiramoto and T. Watanabe, "Experimental Study on RCCV of ABWR Plant, Part 8: Experiments on Liner Anchor and Penetration," *Transaction of the 10th SMiRT Conference*, Vol. J. 1989.

cc:	AE Cubbage	USNRC (with enclosures)
	RE Brown	GEH/Wilmington (with enclosures)
	DH Hinds	GEH/Wilmington (with enclosures)
	EDRF	0000-0083-6330 (RAI 3.8-25 S05)

ENCLOSURE 1

MFN 06-191
Supplement 8

Response to Portion of NRC RAI Letter No. 166
Related to ESBWR Design Certification Application

DCD Tier 2 Section 3.8 – Seismic Category I Structures

RAI Number 3.8-25 S05

For historical purposes, the original text of RAI 3.8-25 and the GEH responses are included. The attachments (if any) are not included from the original responses to avoid confusion.

NRC RAI 3.8-25

Describe how the analysis of a typical liner plate-to-RCCV attachment is performed using the NASTRAN model results. Include this information in DCD Section 3.8.1 and/or Appendix 3G.

In addition, (1) identify the applicable detailed report/calculation (number, title, revision and date, and brief description of content) that will be available for audit by the staff, and (2) reference this report/calculation in the DCD.

GE Response

Rigid bar elements connect the corresponding grid points of the liner elements and concrete elements as described in DCD Appendix 3G.1.4.1. They are schematically shown in Figure 3.8-25(1). To represent the anchor, rigid bar elements are placed in the radial direction for the liners of the RCCV cylinder wall and the RPV pedestal. They are placed vertically for the basemat, the suppression pool slab, and the top slab.

Using this modeling technique, the design forces of liner plates are obtained from the analysis directly, and the anchorage design is performed in accordance with ACI 349-01 Appendix B.

(1) The applicable detailed report/calculation that will be available for NRC audit is 26A6651, RB Structural Design Report, Revision 1, November 2005, containing the structural design details of the Reactor Building.

(2) Since this information exists as part of GE internal tracking system, it is not necessary to add it to the DCD submittal to the NRC.

DCD Impact

No DCD change was made in response to this RAI.

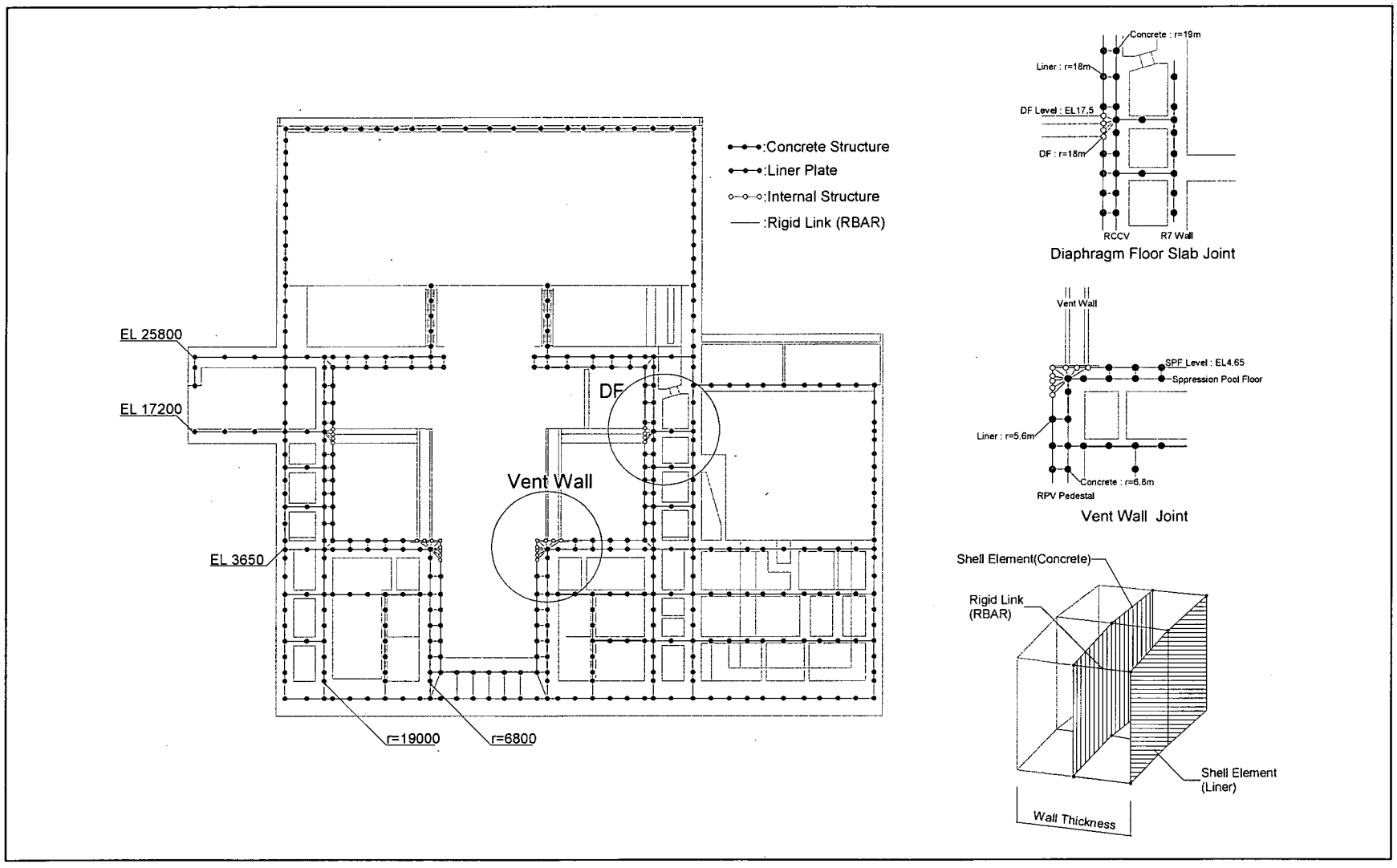

Figure 3.8-25(1) Rigid Bar Elements between Concrete and Liner

NRC RAI 3.8-25 Supplements 1, 2 and 3

Further detailed review needed to fully understand the analysis study performed and to identify specific areas of the description, figures and tables (in the Supplement No. 2 response) which require further clarification. For example, the text indicates that Case 1 is provided to simulate the DCD design technique. However, the table provided for Case 1 - a and -b calls this model "Glued." The DCD and prior discussions with GE seem to indicate that the DCD model is not glued but free to deform between attachment points (rigid links). The concerns raised under this RAI are closely associated with RAI 3.8-26. Additional staff evaluation is also needed to understand the methodology used for analysis of the liner anchors.

During the audit, GE and NRC will need to have a detailed discussion and review - deferred to separate review

GE Response

"Glued" means all concrete and liner nodes are rigidly linked regardless of actual liner anchor locations. This is consistent with the DCD and prior discussions indicating that the DCD model is free to deform between attachment points (nodes).

In order to avoid confusion, the word "glued" used in the NRC RAI 3.8-25, Supplement 2 response is revised to read "DCD," as show in the following "FEM Analysis for Liner Plates" analysis:

FEM ANALYSIS FOR LINER PLATES

1. SCOPE

This analysis provides justification for the adequacy of the modeling technique to correctly predict the behavior of the liner attached to the RCCV wall.

2. ANALYSIS CASES AND MODEL

Two models are provided to predict the behavior of the non-anchored region of the liner plate supported by its anchorage. The non-anchored portion of the plate is coupled to the concrete by rigid link elements or contact elements. The parameters for the analysis are shown on Table 3.8-25(1).

2.1 Analysis cases

Analysis cases are shown in Table 3.8-25(1). Case 1 is provided to simulate the DCD design technique and Case 2 permits the non-anchored region of the liner plate to move in any direction except for the RCCV wall direction.

Table 3.8-25(1) Analysis conditions

Case No.	Model	Coupling with Concrete	Load	Stiffness of Liner
1-a	DCD	Rigid Link	Pressure	E/10000
1-b			Thermal	E
2-a	Contact	Contact spring*[1]	Pressure	E/10000
2-b			Thermal	E

*1; depends on the function of NASTRAN

2.2 Model

The width of the model is twice the Liner anchor pitch (2 x 5.14 degrees) and the height is the half of width. Six degrees of freedom of nodes provided for liner are subordinations to these of RC wall. Figure 3.8-25(2) shows the analysis models.

Coordinate System : Cylindrical, radius = 18m
Size : Liner plate = 6 mm
: Concrete wall thickness = 2 m
Boundary Conditions :
vertical edges : axi-symmetric condition
bottom : simple support [θ, z], but [r] is free
top : for Pressure Load: Same as bottom
: for Thermal Load: Rigid Link
Division : divide the width of Liner anchor pitch (5.14 degrees) into 4 elements

2.3. Material properties

Refer to Table 3.8-25(1). The Young's Modulus is set to a very small value, i.e. 1/10,000 of the standard value, for pressure loads so that the liner resistance to pressure loads will be discounted. For thermal loads, the standard Young's Modulus value is used to account for the effect of differential thermal expansion between steel and concrete.

3. LOADS

Pressure and thermal loads are considered as shown bellow:

Pressure: 45 psig = 0.31 MPa (LOCA after 72 hr)
Thermal: Average temperatures to concrete wall and liner are assigned
Concrete = 20°C
Liner =170°C
Initial temperature = 15.5°C

4. RESULT

Figures 3.8-25(3) and 3.8-25(4) show the strains. The strains are the same for Case 1 and Case 2. Therefore the DCD modeling technique is acceptable.

Table 3.8-25(2) Material Properties

		Reinforced Concrete	Liner
		f'c=5000psi 34.5MPa	Carbon Steel
Young's Modulus (MPa)	Temperature	2.78×10^{4}	2.00×10^{5}
	Pressure	2.78×10^{4}	2.00×10^{1}
Poisson's Ratio		0.17	0.3
Thermal Expansion (m/m°C)		9.90×10^{-6}	1.17×10^{-5}

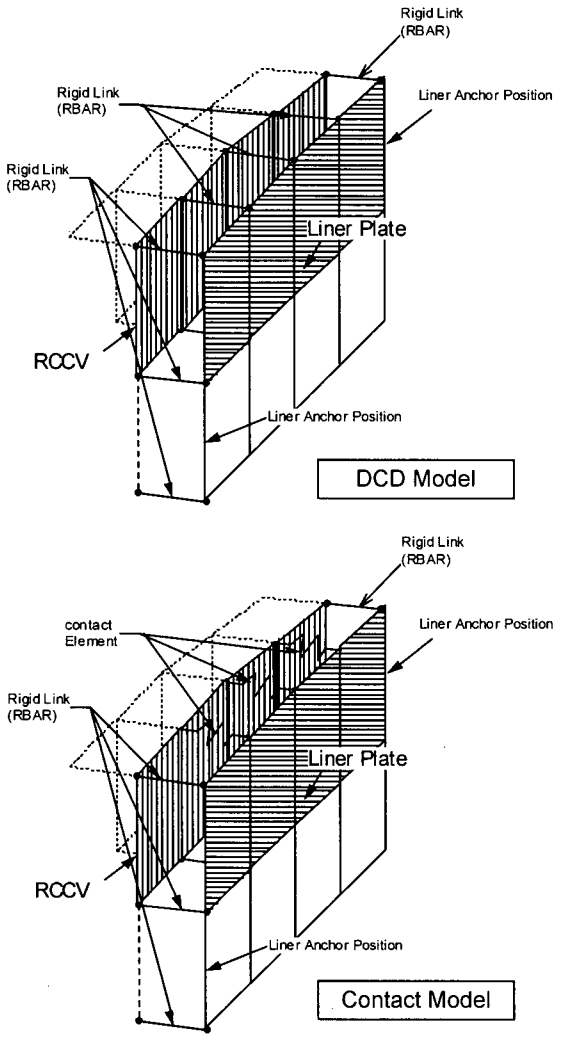

Figure 3.8-25(2) Analysis Models

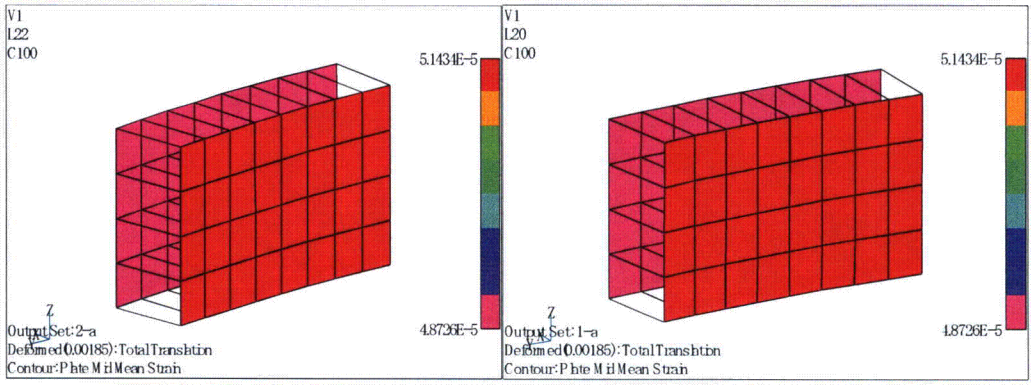

a) DCD Model **b) Contact Model**

Figure 3.8-25(3) Liner Strains (Pressure)

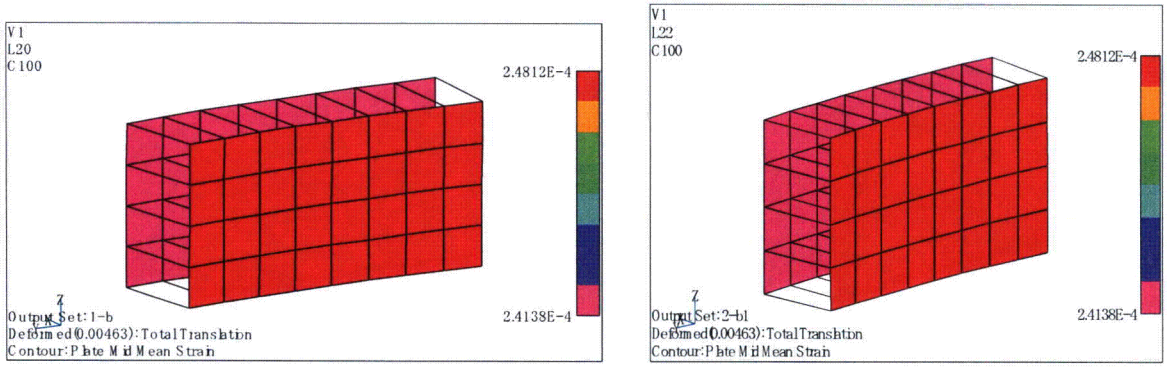

a) DCD Model **b) Contact Model**

Figure 3.8-25(4) Liner Strains (Thermal)

DCD Impact

No DCD change was made in response to this RAI Supplement.

NRC RAI 3.8-25, Supplement 4

NRC Assessment from Chandu Patel E-mail Dated May 24, 2007

From the information provided in the response, it is not clear whether the comparative analysis between the small "DCD Model" and the "Contact Model" addresses this issue. The two models appear to be basically the same, except that each rigid link was replaced by a contact element. Therefore, it is not surprising that the liner strains are the same. The applicant should indicate whether the small DCD Model represents the exact concrete, liner, and rigid link modeling configuration used in the full DCD building model. This should include confirmation of the horizontal and vertical spacing of the rigid links and whether this model represents the most critical location (e.g., where spacings between rigid links are large). Also, from the information provided it is not clear that the existing contact model had a sufficient number of contact elements and liner plate elements (with additional nodes in the plate elements between the contact elements) to properly simulate the true design configuration that will be constructed. The comparison of responses should also include a tabulation of maximum strains (membrane and membrane plus bending) and reaction loads at key liner anchor locations.

GEH Response

1. The small DCD Model represents the exact concrete, liner, and rigid link modeling configuration used in the full DCD Building Model.

   The comparative analyses between the small DCD Model and the Contact Model provided in NRC RAI 3.8-25, Supplement 1, 2 and 3 evaluates the potential for the liner to penetrate the concrete surface in the global FEM model. "DCD Model" means that all liner nodes are connected to concrete nodes with rigid links, which is the same technique as the global FEM model, without consideration of actual liner anchor locations.

2. The section "FEM Analysis for Liner Plates" provided in NRC RAI 3.8-25, Supplement 1, 2 and 3 has been updated as shown in the following section to match the exact upper drywell liner anchor spacing of 1.6^{o} (see DCD Tier 2 Figure 3G.1-48).

   Additionally, to evaluate the mesh size effect, a sensitivity analysis is performed with a refined Contact Model in which the number of contact elements and liner plate elements is twice of that in the existing Contact Model. The results of the refined Contact Model are the same as the original Contact Model as shown below.

3. The membrane strains in the circumferential direction and reaction loads at key liner anchor locations are shown in Tables 3.8-25(5) and (6). The liner anchor reaction forces shown in Table 3.8-25(6) are the internal forces in the rigid links/contact elements located at the center of the models. The liner anchor reactions of the refined Contact Model are one half of the "coarse" Contact Model and DCD Model because the number of contact elements in the refined Contact Model is twice the other two models. Because these models simulate a part of the axi-symmetric cylinder, circumferential forces and bending forces are not induced. The same results obtained from the three models justify the adequacy of the DCD modeling technique for liner anchors.

Even though liner anchor reactions in the circumferential direction are zero in the NASTRAN analysis, liner anchors are designed in accordance with the more severe design conditions as described in the response to NRC RAI 3.8-26.

FEM ANALYSIS FOR LINER PLATES

1. SCOPE

This analysis provides justification for the adequacy of the modeling technique to correctly predict the behavior of the liner attached to the RCCV wall. The results of the analysis provided in NRC RAI 3.8-25, Supplement 1, 2 and 3 have been updated in NRC RAI 3.8-25, Supplement 4 to match the exact upper drywell liner anchor spacing of 1.6^{o} (see DCD Tier 2 Figure 3G.1-48, Section A-A). A refined Contact Model in which the number of contact elements and liner plate elements is twice that in the previous Contact Model is also considered.

2. ANALYSIS CASES AND MODEL

Three models are provided to predict the behavior of the non-anchored region of the liner plate supported by its anchorage. The non-anchored portion of the plate is coupled to the concrete by rigid link elements or contact elements. The parameters for the analysis are shown in Table 3.8-25(3).

2.1 Analysis cases

The analysis cases are shown in Table 3.8-25(3). Case 1 is provided to simulate the DCD design technique and Case 2 permits the non-anchored region of the liner plate to move in any direction except the RCCV wall direction. Case 3 is a refined mesh model of Case 2 to confirm whether a sufficient number is provided for liner and contact elements.

2.2 Model

The width of the model is twice the liner anchor pitch (2 x 1.6 degrees) and the height is the half of the width. Six degrees of freedom of nodes provided for liner are subordinations to these of the RC wall. Figure 3.8-25(5) shows the analysis models. The RCCV wall is modeled in the center of the wall thickness and the liner is placed on the position of the RCCV wall surface.

Coordinate System : Cylindrical, radius = 18 m
Size : Liner plate = 6 mm
: Concrete wall thickness = 2 m
Boundary Conditions :
vertical edges : axi-symmetric condition
bottom : simple support [z], but [θ, r] is free
top : for Pressure Load: Same as bottom
: for Thermal Load: Rigid Link
Division : divide the width of Liner anchor pitch (1.6 degrees) into 4 elements

2.3. Material properties

Refer to Table 3.8-25(4). The Young's Modulus is set to a very small value, i.e. 1/10,000 of the standard value, for pressure loads so that the liner resistance to pressure loads will be discounted. For thermal loads, the standard Young's Modulus value is used to account for the effect of differential thermal expansion between the steel and concrete.

3. LOADS

Pressure and thermal loads are considered as shown bellow:

Pressure: 45 psig = 0.31 MPag (72-hour after LOCA)

Thermal: Average temperatures to concrete wall and liner are assigned

Concrete = 20°C

Liner =170°C

Initial temperature = 15.5°C

4. RESULTS

Table 3.8-25(5) and Figures 3.8-25(6) and (7) show the strains in the circumferential direction. The strains are the same for all cases.

Liner anchor reaction forces shown in Table 3.8-25(6) are the internal forces in the rigid links/contact elements located at the center of the models. Liner anchor reactions of the refined Contact Model are one half of the "coarse" Contact Model and DCD Model because the number of contact elements in the refined Contact Model is twice the other two models. Because these models simulate a part of axi-symmetric cylinder, circumferential forces and bending forces are not induced. The same results obtained from the three models justify the adequacy of the DCD modeling technique for liner anchors.

Table 3.8-25(3) Analysis conditions

No.	Model	Coupling with Concrete	Load	Stiffness of Liner
1-a	DCD	Rigid Link	Pressure	E/10000
1-b			Thermal	E
2-a	Contact	Contact Spring*1	Pressure	E/10000
2-b			Thermal	E
3-a	Contact (refined mesh)	Contact Spring*1	Pressure	E/10000
3-b			Thermal	E

*1; depends on the function of NASTRAN

Table 3.8-25(4) Material Properties

		Reinforced Concrete	**Liner**
		f'c=5000psi 34.5MPa	Carbon Steel
Young's Modulus (MPa)	Temperature	2.78×10^{4}	2.00×10^{5}
	Pressure	2.78×10^{4}	2.00×10^{1}
Poisson's Ratio		0.17	0.3
Thermal Expansion (m/m°C)		9.90×10^{-6}	1.17×10^{-5}

Table 3.8-25(5) Strains of RCCV Wall and Liner

Load	Model		Strains in Circumferential direction	
			RCCV	Liner
Pressure	1-a	DCD	9.746E-5	1.029E-4
	2-a	Contact	9.746E-5	1.029E-4
	3-a	Contact (refined mesh)	9.746E-5	1.029E-4
Thermal	1-b	DCD	2.429E-4	2.564E-4
	2-b	Contact	2.429E-4	2.564E-4
	3-b	Contact (refined mesh)	2.429E-4	2.564E-4

Table 3.8-25(6) Reaction Forces at Liner Anchor

Load	Model		Reaction Forces (MN)	
			Circumferential	Radial
Pressure	1-a	DCD	0.0	-1.948E-02
	2-a	Contact	0.0	-1.948E-02
	3-a	Contact (refined mesh)	0.0	-9.739E-03
Thermal	1-b	DCD	0.0	-1.039E-02
	2-b	Contact	0.0	-1.039E-02
	3-b	Contact (refined mesh)	0.0	-5.195E-03

Note: Reaction forces are at center position of models.

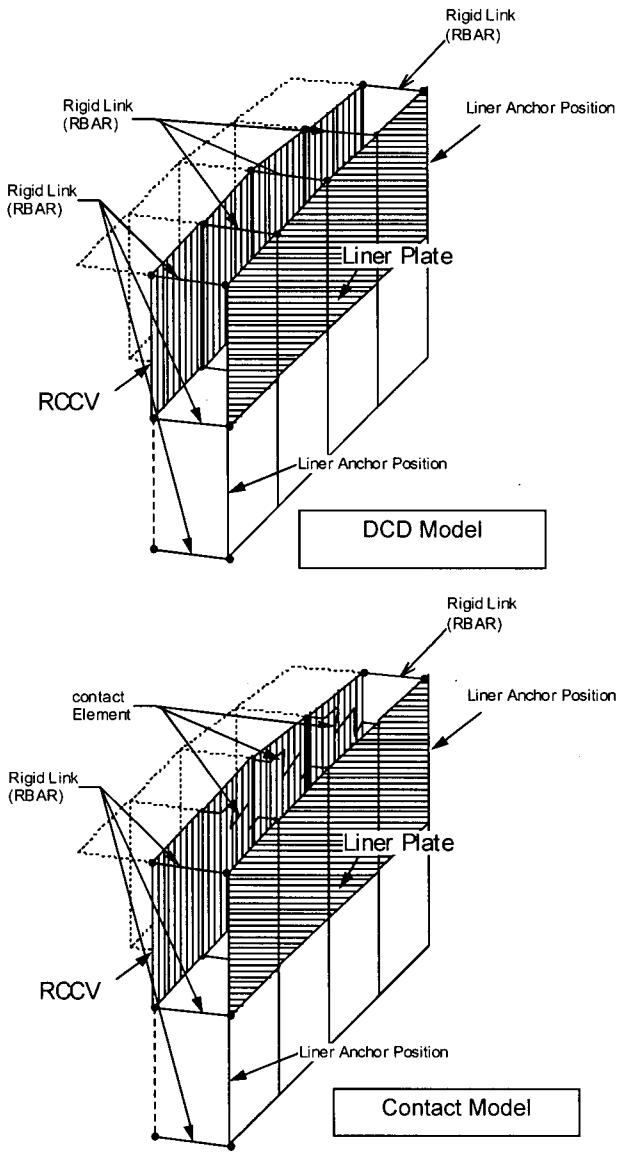

Figure 3.8-25(5) Analysis Models

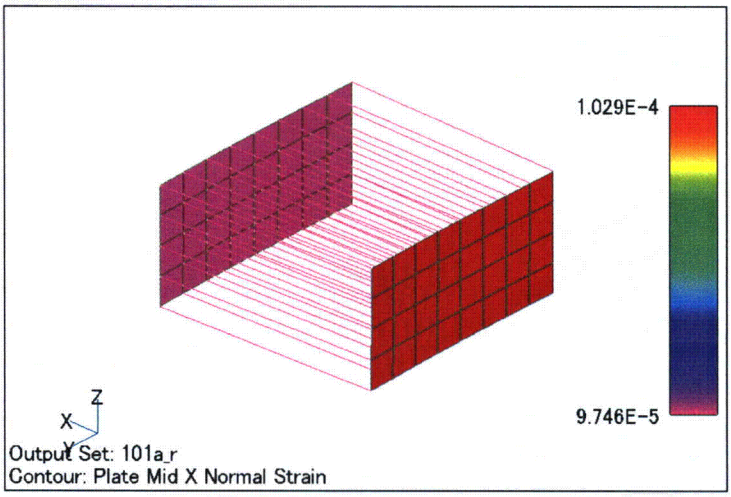

a) DCD Model

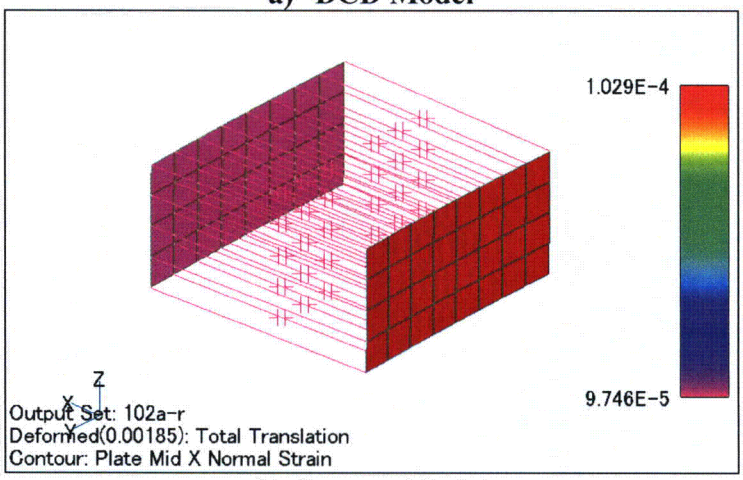

b) Contact Model

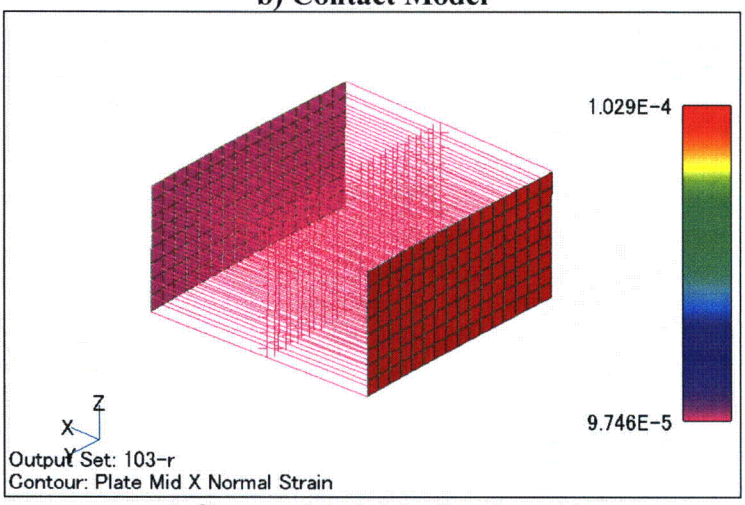

c) Contact Model (refined mesh)

Figure 3.8-25(6) Liner Strains (Pressure)

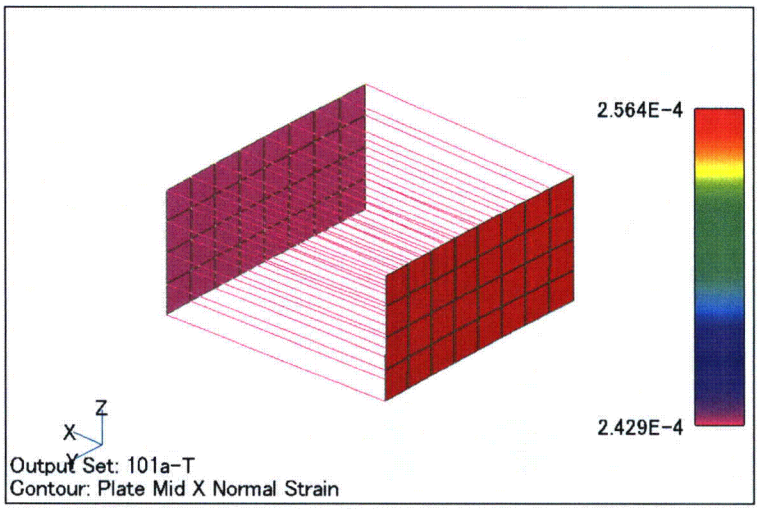

a) DCD Model

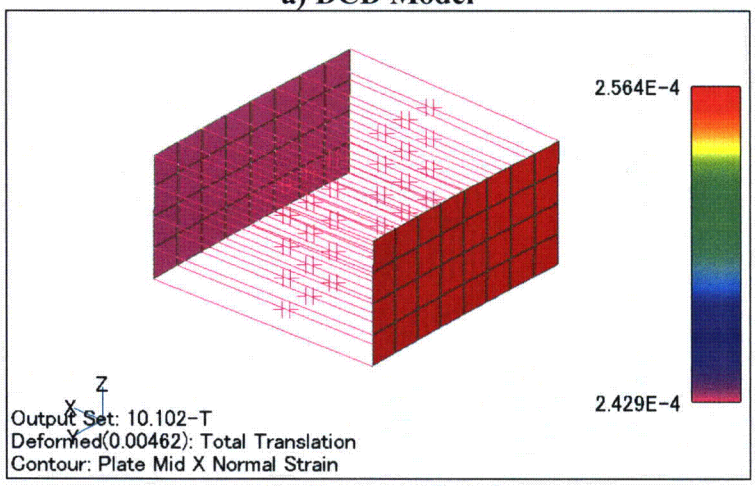

b) Contact Model

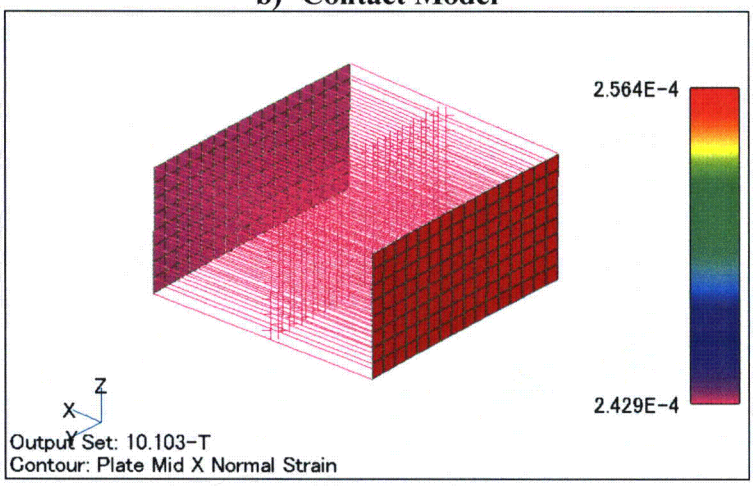

c) Contact Model (refined mesh)

Figure 3.8-25(7) Liner Strains (Thermal)

DCD Impact

No DCD change was made in response to this RAI Supplement.

NRC RAI 3.8-25, Supplement 5

(1) The response, transmitted in GEH letter dated December 12, 2007, provided some information regarding the analysis of the containment liner plate in the full DCD NASTRAN building model. The information provided in the analytical study of a small portion of the containment wall however, did not address the major concerns raised in the RAI. The small "DCD model" was analyzed and compared to the "contact model" which showed the same strains and reaction forces at the liner anchors. However, under pressure loads the two models are essentially identical and so the strains and anchor loads are expected to be the same. This is similarly true for the thermal loading case. Therefore, it does not appear that the study addresses the concerns raised in the RAI.

It was expected that GEH would configure the small DCD model to be identical to the actual full DCD model configuration; that is, it would match the presumed coarser spacing of finite elements with rigid links used in the full DCD model regardless of the actual liner anchor locations. The contact model should then confirm the accuracy of the small DCD model configuration by using a finer discretization (i.e., more finite elements) spaced between the actual locations of the liner anchors. For this contact model, the use of rigid links at the actual anchor locations in both horizontal and vertical directions and the use of contact elements at all other node locations would be acceptable. These two models would not match each other as they do in the current study submitted in the supplemental response.

Based on the above, GEH is requested to revise the analytical models or explain how the current study in the RAI response addresses the potential differences between the current liner model in the full DCD model (which does not match the actual liner anchor spacing and has a presumably coarser distribution) and the true liner configuration with actual anchor spacings.

(2) As part of this RAI, GEH is also requested to provide the following information:

a. How are the strains tabulated in DCD Table 3G.1-35 determined? Are they obtained directly from the individual finite elements of the full DCD NASTRAN model and are they the maximum membrane and maximum membrane plus bending strain acting in any direction throughout the thickness of the liner plate?

b. Since the NASTRAN analysis does not consider potential buckling of the liner plate, GEH is requested to explain if buckling of the liner can occur under the maximum calculated strains for the most critical anchor spacing configuration. If buckling can occur, then describe the calculation performed to obtain the strains in the buckled configuration and demonstrate that they still meet the allowable strain limits in the ASME Code. This should include consideration of the liner strains under thermal local effects on the containment liner due to design basis accident condition. Considering the time-dependent nature of the load, pressure loading may not be present to mitigate the buckling of the liner.

GEH Response

(1) The small DCD model is updated so that it is identical to the actual full DCD model configuration. Figure 3.8-25(8) shows the modeling area for the updated small DCD model extracted from the actual DCD model. The contact model is also updated to cover the same region as the small DCD model. The contact model uses a more refined mesh and takes into account the actual liner anchor locations spaced at 1.6 degrees apart. The entire range of both models is 120 degrees in the circumferential direction with element spacing at 7.5 degrees in the small DCD model and 0.8 degrees in the contact model.

The section "FEM Analysis for Liner Plates" provided in NRC RAI 3.8-25, Supplement 4 has been updated as shown in the section "FEM Analysis for Liner Plates" provided in this RAI response. The same results obtained from both models justify the adequacy of the DCD modeling technique for the liner and liner anchors.

(2)

a. The strains tabulated in DCD Tier 2 Table 3G.1-35 are obtained directly from the individual finite elements of the full DCD NASTRAN model and they are the maximum principal membrane strains. Bending strains of liner plate are very small. For example, membrane plus bending strain that corresponds to the maximum membrane strain of 0.0041 (high-precision number is 0.0040860) at the cylinder for the abnormal/extreme environment category, as shown in DCD Tier 2 Revision 5 Table 3G.1-35, is 0.0040915, so bending strain itself is only 0.0000055. This is 0.13% of membrane strain. And allowable strains for them, shown in ASME Section III, Division 2, Table CC-3720-1, are much larger than those for membrane plus bending strains. Therefore, membrane strains control the liner design.

Solving for ε_b using the following equation demonstrates that bending strains of liner plate are negligibly small: (See Figure 3.8-25(12) for an explanation of the below variables):

$$\varepsilon_b = \frac{(R+t)\cdot\theta - \left(R+\frac{t}{2}\right)\cdot\theta}{\left(R+\frac{t}{2}\right)\cdot\theta} = \frac{t}{2\cdot\left(R+\frac{t}{2}\right)} \approx \frac{t}{2\cdot R} \quad (\because R >> t)$$

where,

ε_b = bending strain at liner surface
R = radius of curvature of RCCV wall inner surface deformation
t = liner plate thickness; t = 6.4 mm
θ = angle of distortion

Since the radius of the RCCV is much larger than the liner thickness, the bending strain of the liner plate, $\varepsilon_b = t/2R$, is negligibly small.

The liner strains calculated from the full DCD NASTRAN model are converted to anchor forces using the standard 2D plane stress equation below:

$$F_H = \sigma_x \cdot t = \frac{E \cdot t}{1 - \nu^2} \cdot \left(\varepsilon_x + \nu \cdot \varepsilon_y\right)$$

where,

F_H = anchor force induced by liner strain
E = modulus of elasticity
t = liner plate thickness
ν = Poisson's ratio
ε_x = strain in the direction perpendicular to anchor
ε_y = strain in the direction perpendicular to ε_x

The anchored forces obtained are then used to determine the anchor displacements in accordance with the load-displacement curve developed from test results of tee anchors in NRC RAI 3.8-25, Supplement 5, Reference 1. A copy of this reference is attached as Attachment 3.8-25(1). The maximum anchor displacements at various locations are summarized in Table 3.8-25(11) and as shown, they are within the allowable limits in ASME Code Table CC-3730-1.

b. To evaluate liner buckling potential under DBA thermal load of 171°C, a separate finite element analysis using ABAQUS computer code is performed for the local liner model shown in Figure 3.8-25(13) for the following two anchor spacing cases: 508 mm (maximum spacing in the design) and 270 mm. The analysis is performed in two steps. The first step is an elastic buckling analysis. The calculated buckling mode shape is then scaled to simulate initial imperfection of the model in a subsequent elasto-plastic stress analysis under the DBA thermal load. The maximum initial imperfection considered is 0.1 mm for both anchor spacing cases. For the 508 mm spacing case, 0.2 mm and 0.64 mm (10% of the liner thickness) initial imperfection are also evaluated and the resulting liner strains are found to be smaller than the 0.1 mm initial imperfection case. The analysis results are shown in Table 3.8-25(10), Figure 3.8-25(14) and Figure 3.8-25(15). Figures 3.8-25(14) and 3.8-25(15) reveal that the liner would buckle when temperature reaches about 80°C and 47°C for the 270 mm and 508 mm anchor spacing, respectively. The maximum liner strains, summarized in Table 3.8-25(10), still meet the allowable limits of ASME Section III, Division 2, Subsection CC-3720.

Reference 1: A. Komori, M. Nazuka, 0. Oyamada, H, Furukawa, M. Hiroshima, Y. Muramatsu, M. Hiramoto and T. Watanabe. "*Experimental Study on RCCV of ABWR Plant, Part 8: Experiments on Liner Anchor and Penetration*". Transaction of the 10th SMiRT Conference, Vol. J. 1989.

FEM ANALYSIS FOR LINER PLATES

1. SCOPE

This analysis provides justification for the adequacy of the modeling technique used in the DCD design to correctly predict the behavior of the liner attached to the RCCV wall.

2. ANALYSIS CASES AND MODEL

2.1 Analysis cases

Analysis cases are shown in Table 3.8-25(7). Case 1, which uses a partial model of the actual DCD model, is provided to simulate the DCD design technique and Case 2 is to simulate more refined liner behavior using rigid links at the actual liner anchor locations and contact elements at non-anchored locations to allow the liner plates to move in any directions except toward the RCCV wall.

2.2 Models

The modeling area is a 120-degree segment of the actual full DCD model as shown in Figure 3.8-25(8). In the small DCD model, the standard width of elements is 7.5 degrees in the circumferential direction and rigid links are used to connect the concrete and liner nodes regardless of the actual anchor locations. A refined element width of 0.8 degrees is used in the contact model, in which rigid links are used only at the actual anchor locations spaced at 1.6 degrees apart and contact elements are used in the non-anchored areas. Figure 3.8-25(9) shows the analysis models. The RCCV wall is modeled in the center of wall thickness and the liner plate is placed at the inner surface of the RCCV wall.

Coordinate System : Cylindrical, radius = 18 m
Size : Liner plate = 6 mm
: Concrete wall thickness = 2 m
Boundary Conditions :
vertical edges : axi-symmetric condition
bottom : simple support [z], but [θ, r] is free
top : for Pressure Load: Same as bottom
: for Thermal Load: free

2.3. Material properties

Refer to Table 3.8-25(8). The Young's Modulus is set to a very small value, i.e. 1/10,000 of the standard value, for pressure loads so that the liner resistance to pressure loads will be discounted. For thermal loads, the standard Young's Modulus value is used to account for the effect of differential thermal expansion between steel and concrete.

3. LOADS

Pressure and thermal loads are considered as shown bellow:

Pressure: 45 psig = 0.31 MPag (72-hour after LOCA)

Thermal: Average temperatures to concrete wall and liner are assigned

Concrete = 20°C

Liner =170°C

Initial temperature = 15.5°C

4. RESULTS

Table 3.8-25(9), Figures 3.8-25(10) and 3.8-25(11) show the strains in the circumferential direction. The strains are the same for both cases. Because these models simulate a part of axi-symmetric cylinder, circumferential forces and bending moments are not occurring. The same results obtained from both models justify the adequacy of the DCD modeling technique for liner anchors.

Table 3.8-25(7) Analysis Conditions

No.	Model	Coupling with Concrete	Load	Stiffness of Liner
1-a	small DCD	Rigid Link	Pressure	E/10000
1-b			Thermal	E
2-a	Contact	Contact Spring*[1]	Pressure	E/10000
2-b			Thermal	E

*1; depends on the function of NASTRAN

Table 3.8-25(8) Material Properties

		Reinforced Concrete	**Liner**
		f'c=5000psi 34.5MPa	Carbon Steel
Young's Modulus (MPa)	Temperature	2.78×10^{4}	2.00×10^{5}
	Pressure	2.78×10^{4}	2.00×10^{1}
Poisson's Ratio		0.17	0.3
Thermal Expansion (m/m°C)		9.90×10^{-6}	1.17×10^{-5}

Table 3.8-25(9) Strains of RCCV Wall and Liner

Load	Model		Strains in Circumferential direction	
			RCCV	Liner
Pressure	1-a	small DCD	9.73E-5	1.027E-4
	2-a	Contact	9.75E-5	1.029E-4
Thermal	1-b	small DCD	1.980E-4	2.090E-4
	2-b	Contact	1.980E-4	2.090E-4

Table 3.8-25(10) Buckling Analysis Results Summary

Analysis Model		Max. Reaction Force @ Model Edge (N/mm)	Out-of plane Displacement @ Model Center (mm)	Strain @ Model Center		
					Membrane + Bending	
Anchor Spacing (mm)	Max. Initial Imperfection (mm)			Membrane (Compression)	Tension	Compression
270	0.1	1399	5.4	0.00216	0.0041	0.0084
508	0.1	710	14.8	0.00017	0.0045	0.0049
Allowable Limits of Strain for Factored Load Case				0.005	0.010	0.014

Table 3.8-25(11) Summary of Liner Anchor Displacement Evaluation

Location	Anchor Stiffness	Category I (1)		Category II (2)	
		Displacement (mm)	Allowable (mm)	Displacement (mm)	Allowable (mm)
Wetwell Cylinder (3)	Nominal	0.226	1.27	-	2.54
	Lower	0.357		-	
	Upper	0.171		-	
Pedestal Cylinder (4)	Nominal	-		1.62	
	Lower	-		1.85	
	Upper	-		1.52	
Wetwell Bottom	Nominal	0.250		1.26	
	Lower	0.384		1.50	
	Upper	0.192		1.17	

Notes:
(1) Test, normal, severe environmental and extreme environmental load combinations.
(2) Abnormal, abnormal/severe environmental, and abnormal/extreme environmental load combinations.
(3) Wetwell cylinder displacements for Category II are non-controlling.
(4) Pedestal cylinder displacements for Category I are non-controlling.

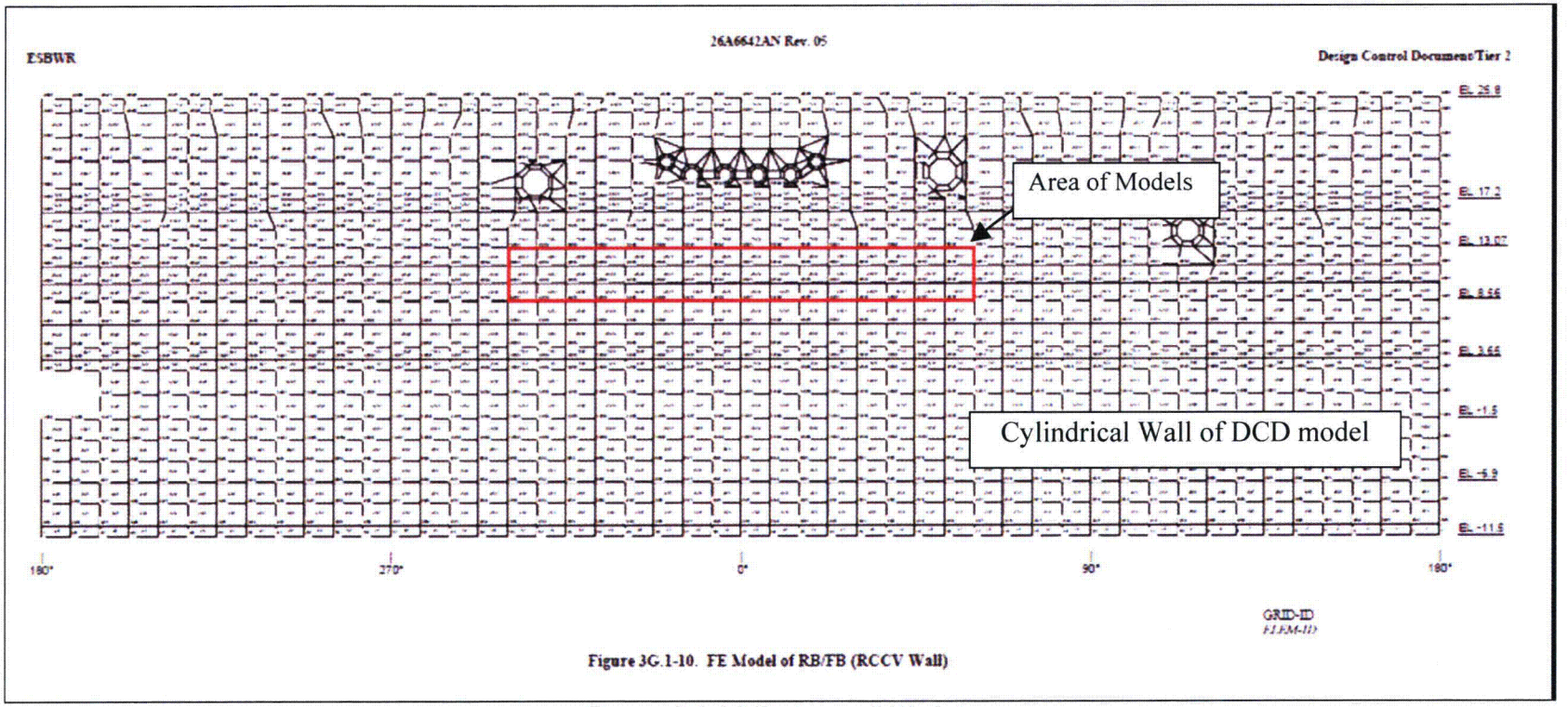

Figure 3.8-25(8) Area of Models

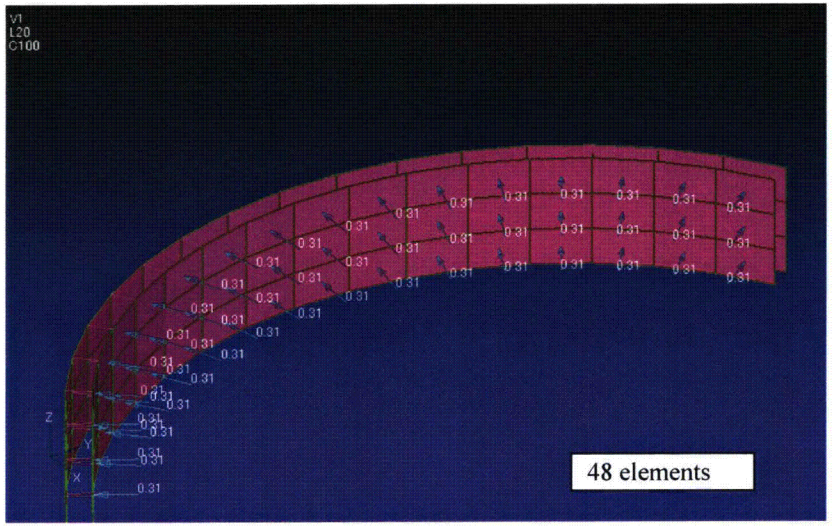

1) Small DCD Model (7.5° pitch)

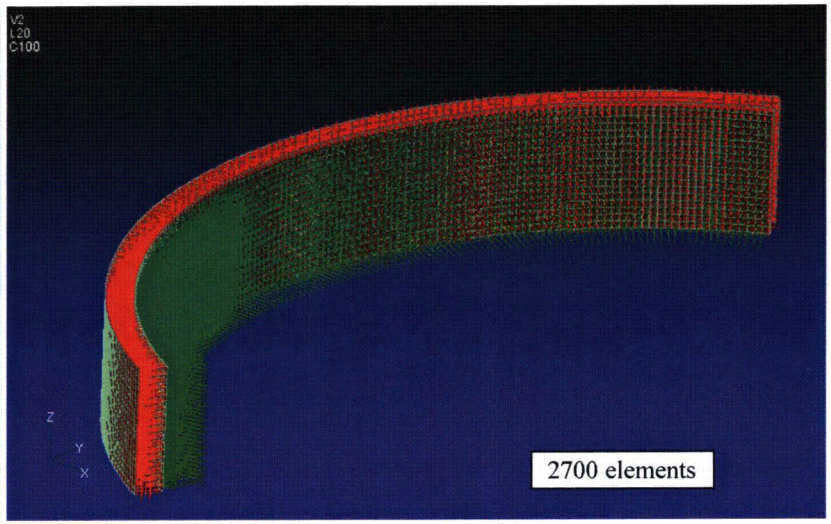

2) Contact Model (0.8° pitch)

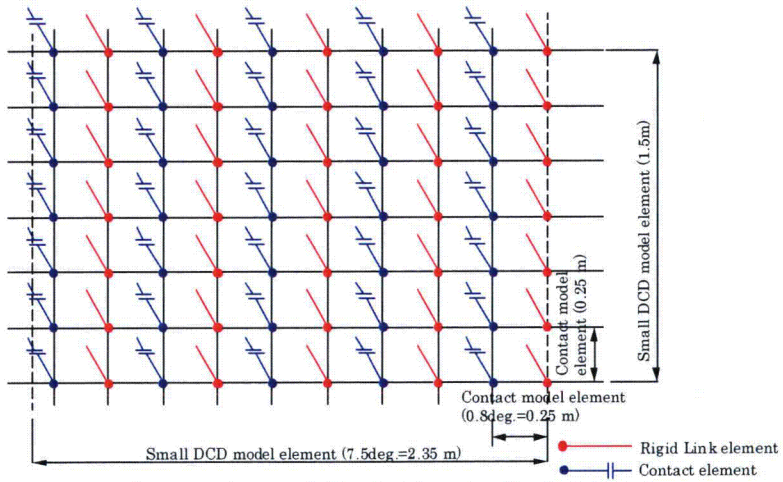

3) Comparison of Mesh Size for Both Models

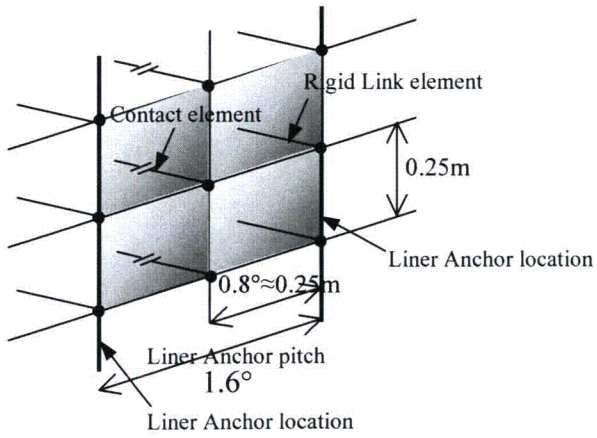

4) Detail of Contact Model (0.8° pitch)

Figure 3.8-25(9) Analysis Models

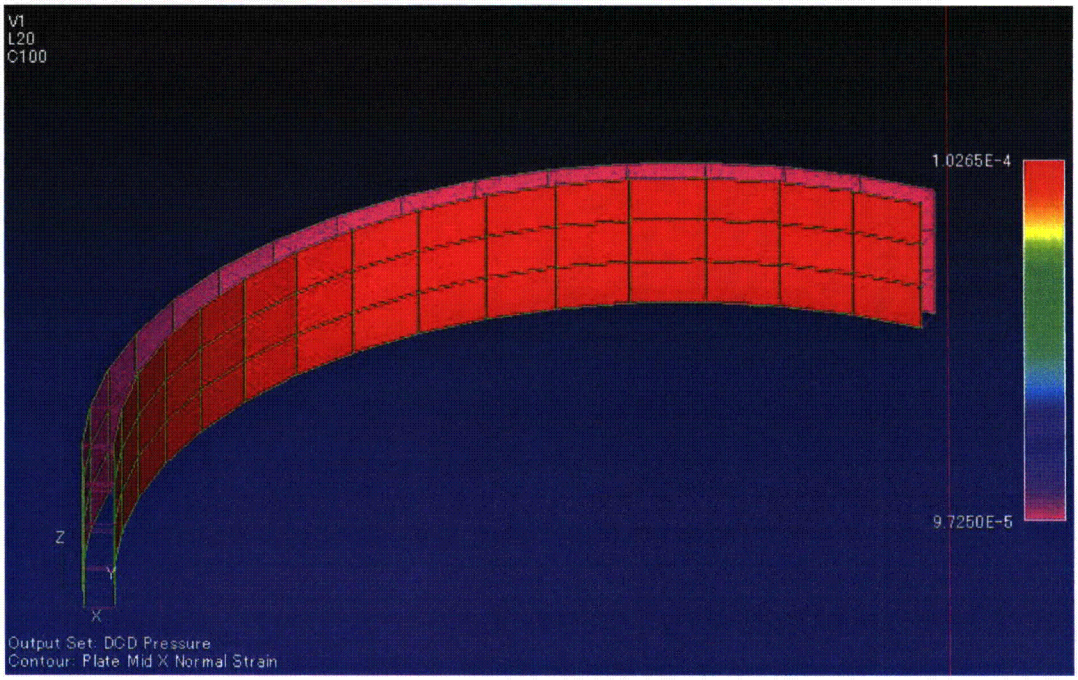

a) Small DCD Model

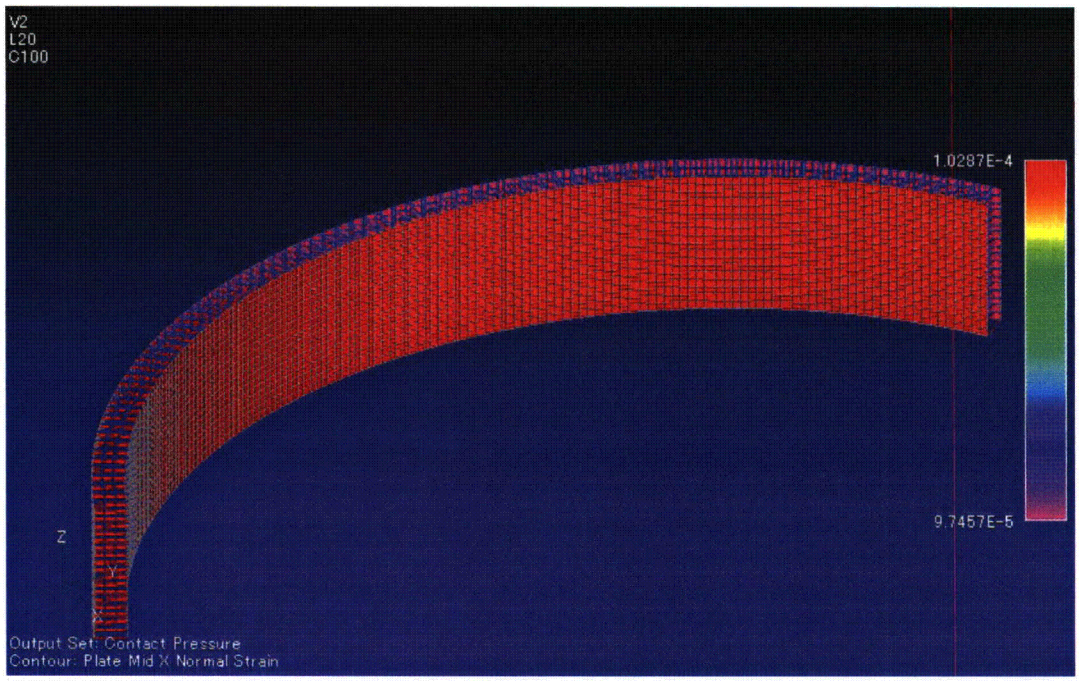

b) Contact Model

Figure 3.8-25(10) Liner Strains (Pressure)

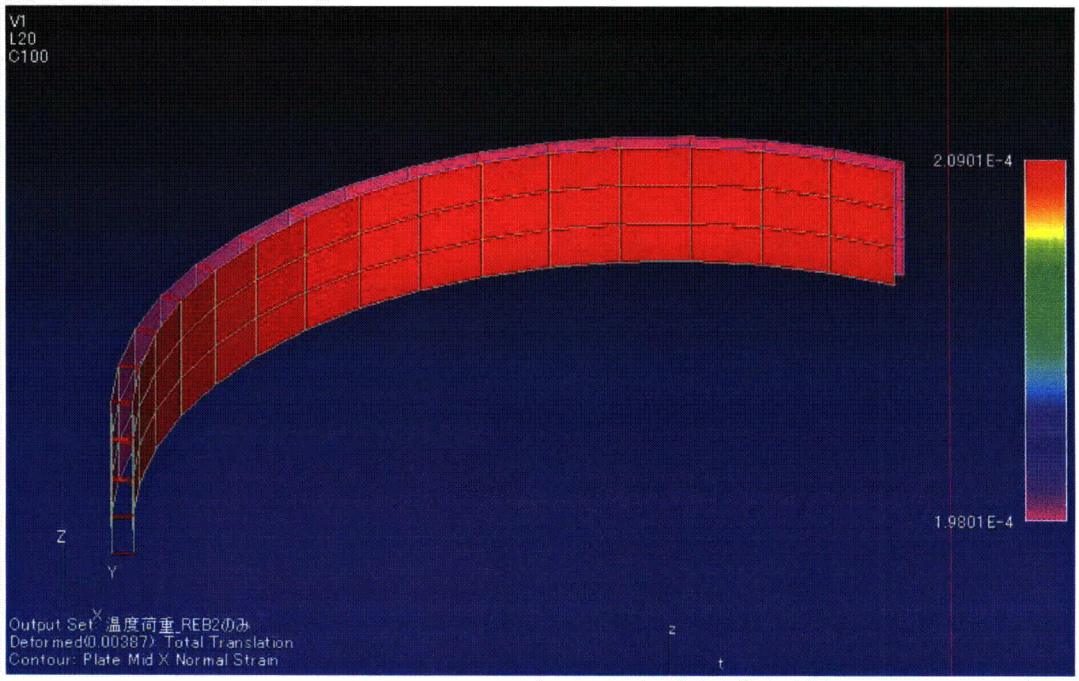

a) Small DCD Model

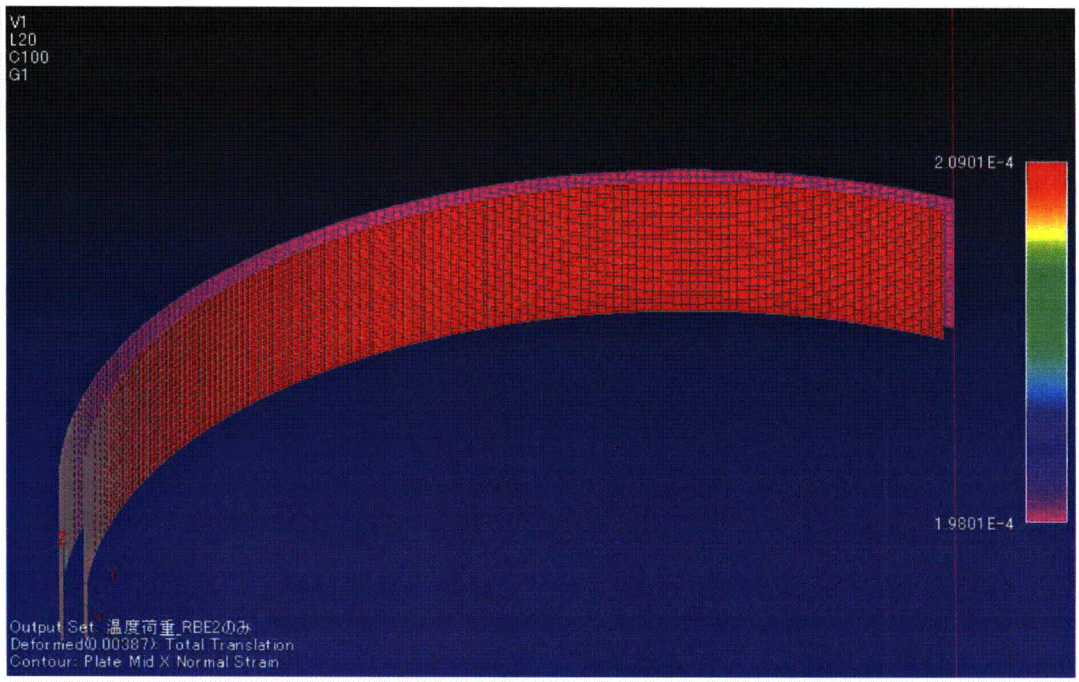

b) Contact Model

Figure 3.8-25(11) Liner Strains (Thermal)

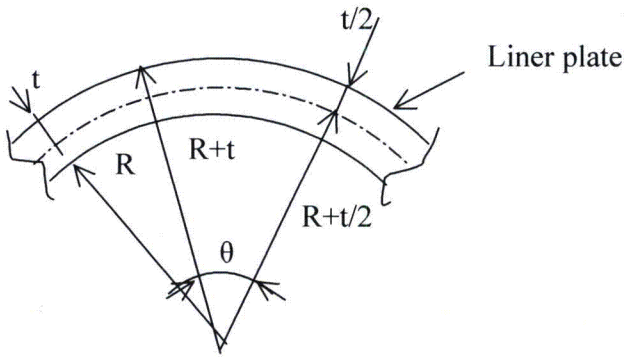

Figure 3.8-25(12) Bending Strain of Liner Plate

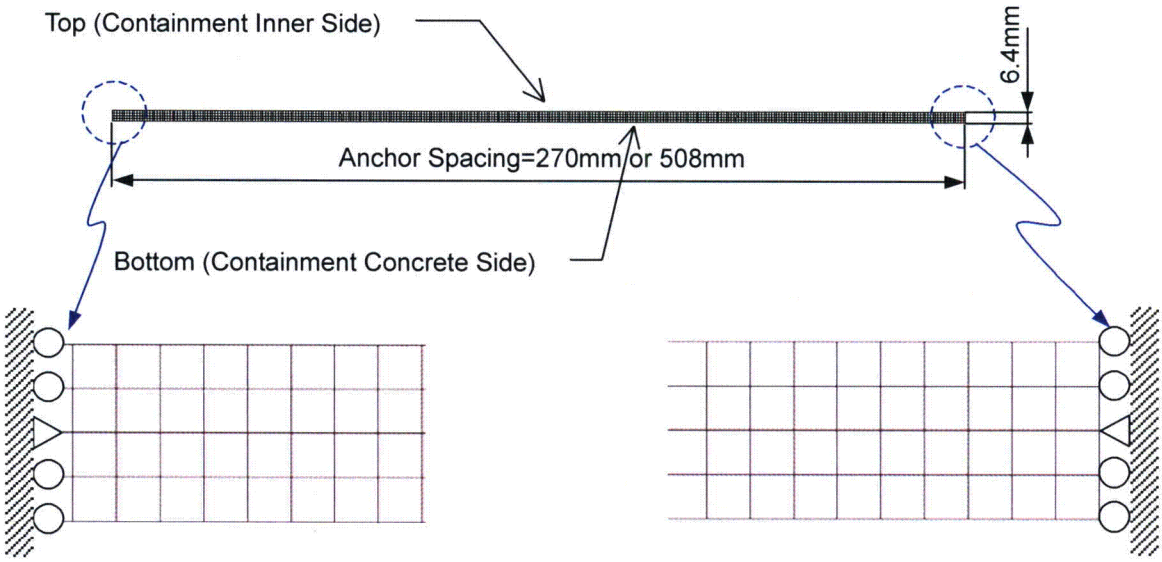

Boundary condition at the analysis model edge

Figure 3.8-25(13) Analysis Model (4 Nodes Plane Strain Element)

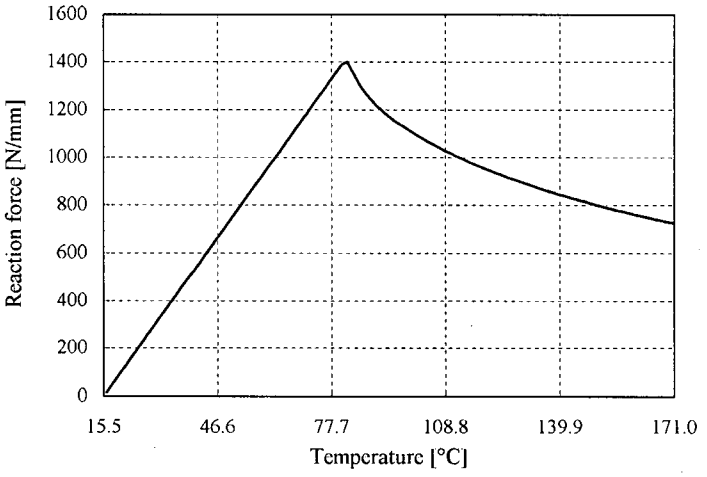

(1) Reaction force at model edge

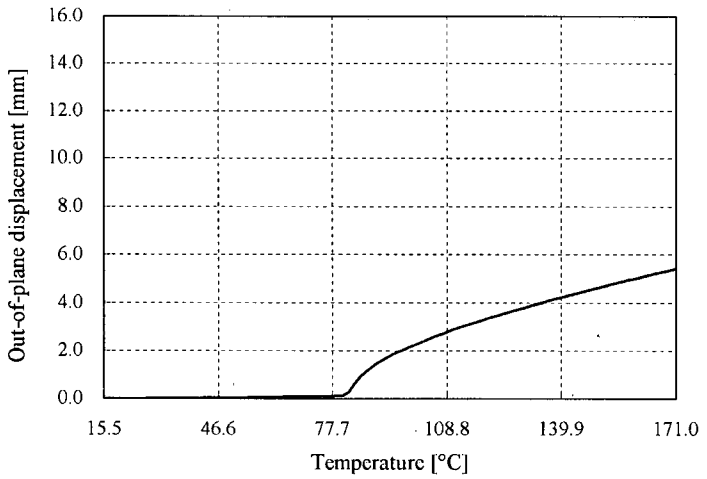

(2) Out-of-plane displacement at model center

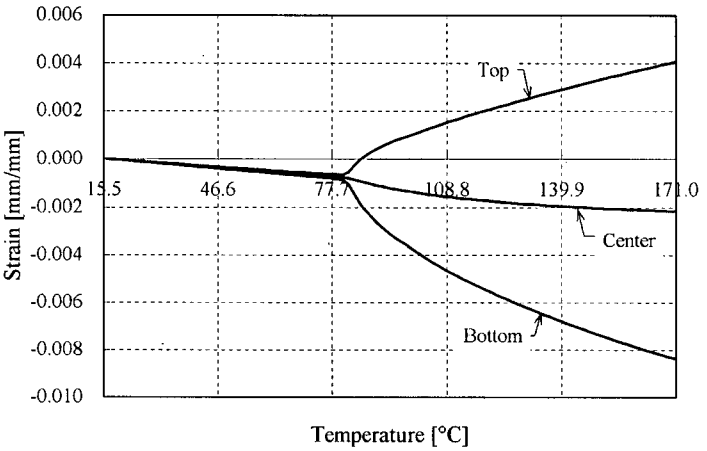

(3) Liner strain at model center

Figure 3.8-25(14) Buckling Analysis Results for 270 mm Anchor Spacing

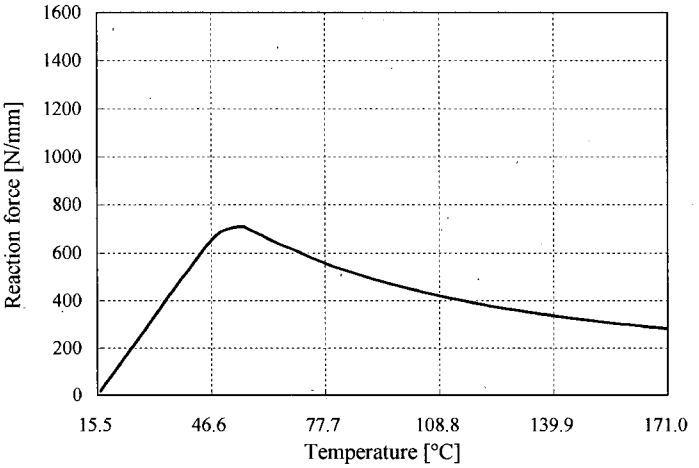

(1) Reaction force at model edge

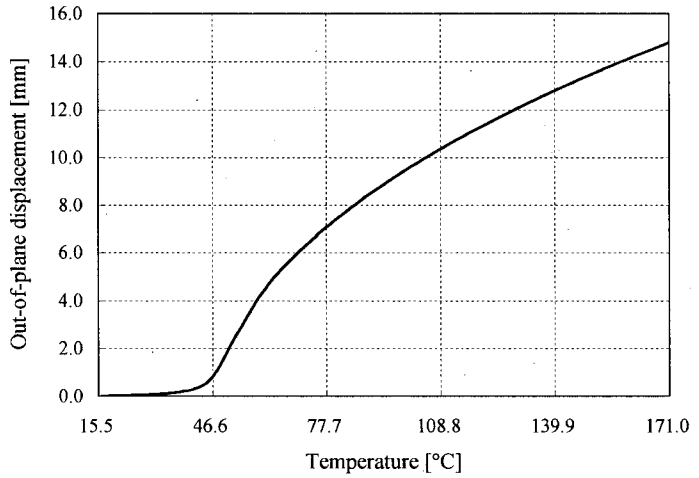

(2) Out-of-plane displacement at model center

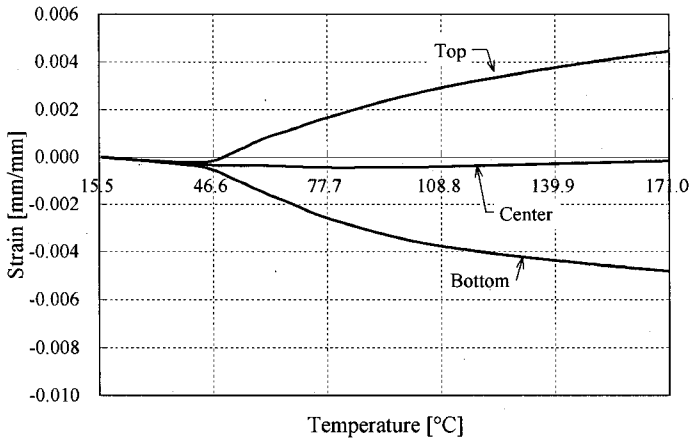

(3) Liner strain at model center

Figure 3.8-25(15) Buckling Analysis Results for 508 mm Anchor Spacing

DCD Impact

No DCD change is required in response to this RAI Supplement.

Attachment 3.8-25(1)

A. Komori, M. Nazuka, 0. Oyamada, H, Furukawa, M. Hiroshima, Y. Muramatsu, M. Hiramoto and T. Watanabe. "*Experimental Study on RCCV of ABWR Plant, Part 8: Experiments on Liner Anchor and Penetration*". Transaction of the 10th SMiRT Conference, Vol. J. 1989

Experimental Study on RCCV of ABWR Plant
Part 8: Experiments on Liner Anchor and Penetration

Akio Komori, Masafumi Nazuka
Tokyo Electric Power Company, Tokyo, Japan
Osamu Oyamada, Hideyasu Furukawa
Hitachi Ltd., Hitachi, Japan
Minoru Hiroshima
Hitachi Ltd., Tsuchiura, Japan
Yutaka Muramatsu, Makoto Hiramoto
Toshiba Corporation, Yokohama, Japan
T. Watanabe
Ishidawajima-harima Industries Company, Ltd., Yokohama, Japan

1. INTRODUCTION

This paper summarizes the study of shear load and deformation characteristics of continuous tee liner plate anchors, and the study of high temperature pipe penetrations in RCCV (Reinforced Concrete Containments Vessel). The major design conditions which produce liner compression and tention are the strain imposed by the overall deformations of the containment and the strain due to thermal expansion of the liner plate itself. These compressive strains can cause large unbalanced loads in the liner plate which result in shear forces acting on the liner plate anchors at geometric discontinuities. Shear force versus deformation test data are necessary to assure that the design is adequate under the ocnditions of deformation and maximum unbalanced load. Objectives of the shear force test for liner anchors are as follows.

(1) To determine the characteristics of the load-deflection curve of the liner anchor.
(2) To develop idealized load-deflection curves for design, based on studies of those characteristic.

Concrete temperature around the high temperature pipe penetration of RCCV is limitted in the Technical Standard on Concrete Containments for Nuclear Power Plats(Draft) of Japan. This limit is the same as in ASME Sec.Ⅱ Div.2. Because strength of the concrete and other characteristics will change within the range of high temperature. Therefore, it is necessary to confirm that concrete temperature around the penetrations are bellow the temperature limits to assure the soundness of concrete. Objectives of the thermal loading tests of high temperature pipe penetration are as follows.

(3) To confirm the adequacy of the method of the calculation and boundary conditions for the temperature distribution analysis.
(4) To confirm that the temperature of concrete around the high temperature pipe penetration in actual plant is bellow the temperature limit of concrete during normal operation.

2. SHEAR TEST OF LINER ANCHOR

2.1 Test specimen and method

The test set-up of the liner anchor specimens is shown in Fig-1. Thickness of the liner plate is 6.4mm SGV49(JIS G3118), corresponding to ASME SA-516(1979) Gr.70, a medium carbon steel, and the liner anchors is tee-shaped, 75x75x6x9 and 100x100x6.5x10, SM 50. The liner plates are placed at both sides of all specimens, symmetrically about the centerline. Liner anchor sizes and the number of tee anchors are shown in Table-1. The spacing of anchors is 500mm in two anchor specimens. The concrete used for the test specimens has a maximum size aggregate of 25mm and an average slump of 8~10cm. The compressive strength of the concrete, poured under construction conditions, not typical laboratory conditions, is from 267kgf/cm^2 to 335kgf/cm^2 at 4 weeks.

A shear force is applied to the specimens by pulling the liner plates, and

displacement of the liner anchors and stresses are measured. Furthermore, since maximum load is related to concrete cracking in some way, the cracks were observed at every step.

2.2 Results

Test results are summarized in Fig-2 through Fig-7.

(1) Maximum load

Maximum loads are different for one anchor specimens and two anchor specimens; with two anchor specimens producing lower loads. In case of the 75x75 tee, the maximum loads are in the range between 62tf to 71tf, while the displacements range from 2mm to 3mm in one anchor specimens (1-1 and 1-2). The maximum laods for two anchor specimens (2-1 and 2-2) range from 50tf to 65tf, while the displacements range from 0.6mm to 1.5mm. The maximum loads for the two anchor specimens are lower than those of one anchor specimens without regard to the size of liner anchor.

(2) Maximum displacement

Displacement of all specimens reaches about 5mm. As with loads, the maximum displacements of two anchor specimens are also lower than those of one anchor specimens.

(3) Cracks in concrete

Typical crack patterns around the liner anchor for one anchor and two anchor specimens are shown in Fig-2 and 3. Cracks around the first anchor in two anchor specimens are different from those in one anchor specimens.

- Slopes of the cracks behind the first anchor are gentle in the two anchor specimens, compared with those of the one anchor specimens.
- Cracks in front of the first anchor are longer than those of one anchor specimens.

Furthermore, it is characteristic in the two anchor specimens that cracks in the front of second anchor slope gently and extend to near the first anchor.

3. THERMAL LOADING TESTS OF HIGH TEMPERATURE PIPE PENETRATIONS

3.1 Test specimen and method

A test specimen of high temperature pipe penetration consists of inner process pipe, outer sleeve, anchor ring and gussets, and is anchored in RCCV. The size of the process pipe and sleeve is based on the penetrations which have been put into actual use, and the diameter of the process pipe and sleeve are 165mm and 508mm, respectively. The process pipe is covered by insulation. The length from the top of the sleeve to RCCV is 1200mm, based on the preliminary study of temperature distribution calculation to keep the ocncrete temperature limits. The model size is decided considering the range to have no effects on the temperature distribution.

A heater is installed inside the process pipe to make normal operating thermal conditions, and an environment box is set outside and inside of RCCV in order to control the temperature of inside of RCCV and R/B respectively. The test specimen and testing apparatus are shown in Fig-8.

3.2 Results

In this experiment, concrete temperature in the vicinity of penetration outside of RCCV was 62°C in maximum as shown in Fig-9. Analysis of temperature distribution, which simulate the experiment, was carried out and its results are shown in Fig-10. The test results and analysis results are relatively in good agreement in comparison with Fig-9 and 10. Therefore, it was confirmed that analysis method, including boundary conditions, of temperature distribution around penetration is reasonable.

To calculate the temperature distribution around the Main Steam (M/S) pipe penetration, whose temperature conditions are severest in high temperature penetrations of actual plant, the analysis model shown in Fig-11 was developed based on the analysis model which simulates the experiment. From the analysis result as shown in Fig-12, it was confirmed that concrete temperature around high temperature penetration is bellow 90°C, which is the limit of applicable

temperature during normal operation of RCCV.

4. CONCLUSION

Results for the two anchor specimens indicate that the maximum load is lower and the stiffness in the initial, or elastic portion of the curve is higher than for the one anchor specimens. In considering this result, it is important to investigate cracking in concrete at maximum load. From investigation of the cracks, the maximum load of the two anchor specimens occures as the crack propagating from the second anchor's flange reaches the first anchor. If the strength of the anchor in shear can be defined as the combined compression and shear strength of the surrounding concrete, the first anchor's strength is supposed to be reduced since its upward restraint by the second anchor is weekened by the crack extending from the second to first anchor. It can be said that the maximum load of the first anchor is affected by the cracks from the rear anchor and is consequently lower than that of one anchor specimens. Therefore, idealized load-deflection curve for design of liner anchors will be set considering primarily the results of the two anchor specimens, to be conservative.

From thermal loading tests of high temperature pipe penetration, it was confirmed that the method and boundary conditions of temperature analysis around high temperature penetration was adequate by comparing test results and analysis results. Using these method and conditions, it was confirmed that concrete temperature around the M/S pipe penetration whose temperature is severest was estimated and bellow the temperature limit of concrete during normal operation.

5. ACKNOWLEDGEMENT

This study has been carried out as a part of a joint research study on "Evaluation of the RCCV Configuration and Comfirmatory Test to Establish a Code"

6. REFERENCE

1) Saito,H., Kikuchi.R., Muramatu,Y., Hiramoto,M., Oyamada,O., Furukawa,H., Sasagawa,K., Ohmori,N., Suzuki,S., Sugita,M., Kobayashi,I., Yamaguchi,I. (1989). Experimental Study on RCCV of ABWR Plant Part 1; Outline of Research Study. Transaction of the 10th SMIRT Conference. Vol. J.

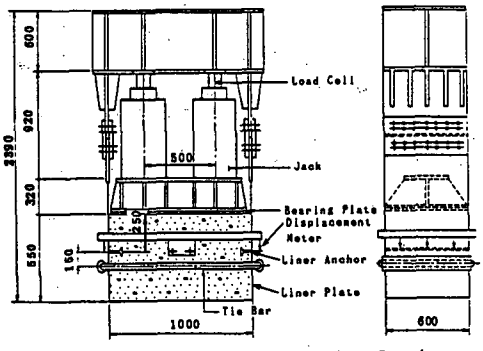

Fig-1 Test Set-up for One Anchor Specimen

Specimen		Anchor Size	No. of Anchor	Age (days)	Strength (kg/cm²)	Young's Modulus (kg/cm²)
1	1-1	CT75×75×6×9	1	39	275	2.21×10⁵
	1-2	CT75×75×6×9	1	61	276	(2.13×10⁵)
2	2-1	CT75×75×6×9	2	33	267	2.13×10⁵
	2-2	CT75×75×6×9	2	40	243	2.45×10⁵
3	3-1	CT100×100×6.5×10	1	28	335	2.46×10⁵
	3-2	CT100×100×6.5×10	1	41	276	2.87×10⁵
4	4-1	CT100×100×6.5×10	2	34	317	2.56×10⁵
	4-2	CT100×100×6.5×10	2	38	276	2.60×10⁵
5	5-1	L75×75×6×9	1	34	249	(2.42×10⁵)
	5-2	L75×75×6×9	1	38	253	2.18×10⁵

Table-1 Description of Specimens

Load

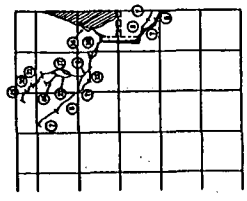

Fig-2
Crack Pattern of One Anchor Specimen

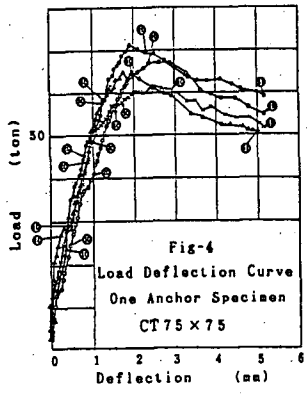

Fig-4
Load Deflection Curve
One Anchor Specimen
CT75×75

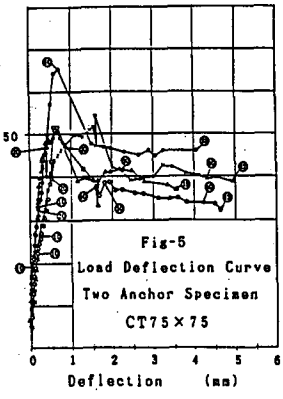

Fig-5
Load Deflection Curve
Two Anchor Specimen
CT75×75

Load

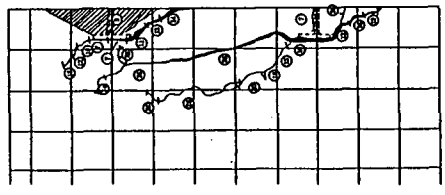

Fig-3
Crack Pattern of Two Anchor Specimen

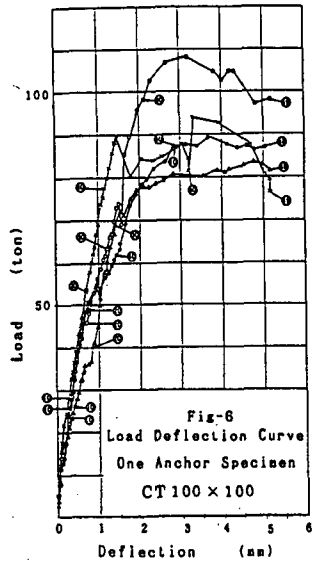

Fig-6
Load Deflection Curve
One Anchor Specimen
CT100×100

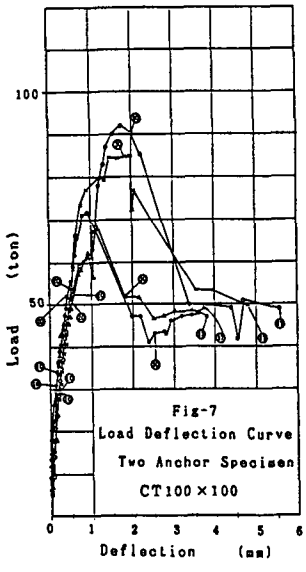

Fig-7
Load Deflection Curve
Two Anchor Specimen
CT100×100

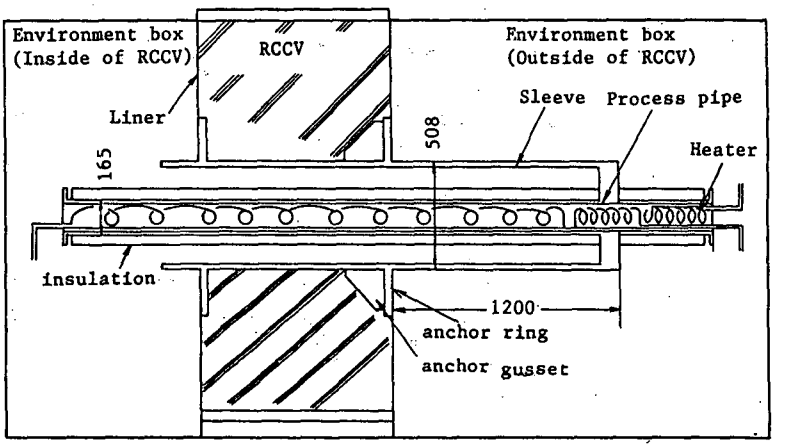

Fig-8 Testing apparatus and test specimen

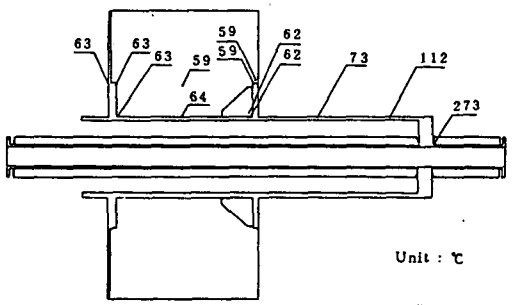

Fig-9 Test results of penetration temperature of test specimen

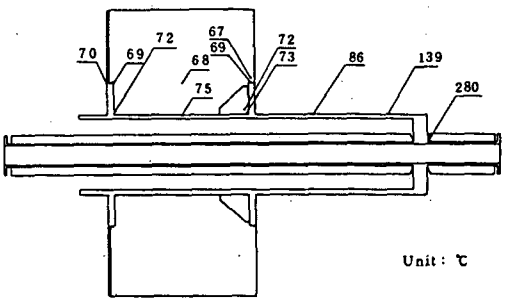

Fig-10 Calculation results of penetration temperature of test specimen

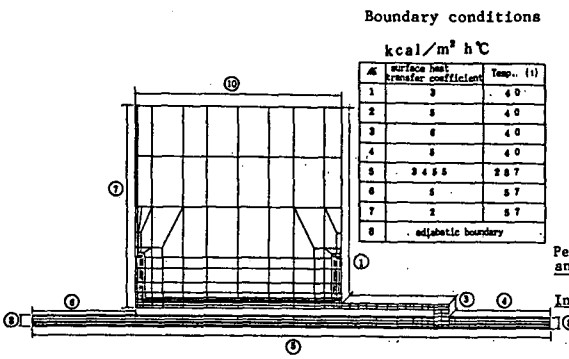

Fig-11 Calculation model and conditions of M/S pipe penetration

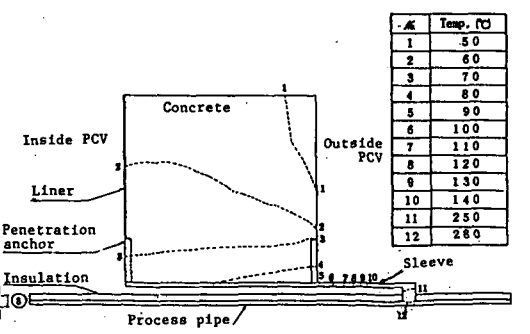

No.	Temp. (℃)
1	50
2	60
3	70
4	80
5	90
6	100
7	110
8	120
9	130
10	140
11	250
12	280

Fig-12 Calculation results of M/S pipe penetration